

RESEARCH ARTICLE

10.1002/2014JC010229

Temporal variations in air-sea CO₂ exchange near large kelp beds near San Diego, CaliforniaHiroki Ikawa^{1,2} and Walter C. Oechel¹¹Global Change Research Group, San Diego State University, San Diego, California, USA, ²International Arctic Research Center, University of Alaska, Fairbanks, Alaska, USA

Key Points:

- One of the first multiyear coastal CO₂ flux monitoring is presented
- CO₂ uptake was observed likely due to kelp growth
- Accurate CO₂ flux measurements over kelps update the global carbon estimate

Supporting Information:

- Readme
- Flux_data

Correspondence to:

H. Ikawa,
hikawa.biomet@gmail.com

Citation:

Ikawa, H., and W. C. Oechel (2015), Temporal variations in air-sea CO₂ exchange near large kelp beds near San Diego, California, *J. Geophys. Res. Oceans*, 120, 50–63, doi:10.1002/2014JC010229.

Received 10 JUN 2014

Accepted 12 DEC 2014

Accepted article online 19 DEC 2014

Published online 13 JAN 2015

Abstract This study presents nearly continuous air-sea CO₂ flux for 7 years using the eddy covariance method for nearshore water near San Diego, California, as well as identifying environmental processes that appear to control temporal variations in air-sea CO₂ flux at different time scales using time series decomposition. Monthly variations in CO₂ uptake are shown to be positively influenced by photosynthetically active photon flux density (PPFD) and negatively related to wind speeds. In contrast to the monthly scale, wind speeds often influenced CO₂ uptake positively on an hourly scale. Interannual variations in CO₂ flux were not correlated with any independent variables, but did reflect surface area of the adjacent kelp bed in the following year. Different environmental influences on CO₂ flux at different temporal scales suggest the importance of long-term flux monitoring for accurately identifying important environmental processes for the coastal carbon cycle. Overall, the study area was a strong CO₂ sink into the sea (CO₂ flux of ca. $-260 \text{ g C m}^{-2} \text{ yr}^{-1}$). If all coastal areas inhabited by macrophytes had a similar CO₂ uptake rate, the net CO₂ uptake from these areas alone would roughly equal the net CO₂ sink estimated for the entire global coastal ocean to date. A similar-strength CO₂ flux, ranging between -0.09 and $-0.01 \text{ g C m}^{-2} \text{ h}^{-1}$, was also observed over another kelp bed from a pilot study of boat-based eddy covariance measurements.

1. Introduction

Globally, the ocean takes up about 1.0–2.2 Pg C of carbon annually [Sabine *et al.*, 2004; Gruber *et al.*, 2009; Takahashi *et al.*, 2009]. This amount represents roughly 25–30% of anthropogenically released CO₂ into the atmosphere [Sarmiento *et al.*, 2000; Takahashi *et al.*, 2002, 2009; Sabine *et al.*, 2004; Gruber *et al.*, 2009]. However, these amounts exclude estimates for the coastal seas due to a lack of information regarding the coastal carbon cycle. Chen and Borges [2009] compiled air-sea CO₂ flux (hereafter, CO₂ flux) data over various coastal ecosystems, concluding that coastal oceans account for about 30% of net CO₂ uptake from the global ocean, while comprising only 6–7% of the global ocean surface. Despite the potential importance of coastal seas for the global carbon cycle, current estimates of the carbon budget of the coastal sea vary by 50% or more [Tsunogai *et al.*, 1999; Thomas, 2004; Borges, 2005; Cai *et al.*, 2006; Chen and Borges, 2009]. The uncertainty in these estimates is attributed mainly to high temporal and spatial heterogeneity in coastal characteristics and inadequate sampling sites. For a better estimate of CO₂ flux over coastal seas, it is necessary to identify the major coastal processes that control the patterns and magnitudes of coastal CO₂ flux.

Macrophytes, such as large kelp and seagrass species, inhabit most temperate coastal areas [Whittaker and Likens, 1973; Dayton, 1985]. While they inhabit only about 1% of the ocean surface (about $2 \times 10^6 \text{ km}^2$), their high productivity strongly influences regional carbon cycles [Delille *et al.*, 1997, 2000; Wilmers *et al.*, 2012]. The turnover rate of macrophytes is not as fast as phytoplankton, such that new production can be effectively enhanced. The amount of primary production of the macrophytes over the globe is estimated to be about 1 Pg C yr⁻¹, representing half the carbon uptake by the global ocean [Smith, 1981]. However, it is still not well understood to what extent the net primary production affects air-sea CO₂ transfer. The quantification of CO₂ flux over macrophyte ecosystems is limited, mainly due to technical difficulties. The bulk method is used widely to estimate CO₂ flux in the world open ocean [Takahashi *et al.*, 2009], though the application of this method over macrophyte ecosystems still remains challenging due to uncertainty in the air-sea gas transfer property [Delille *et al.*, 2009].

Since the development of the eddy covariance (EC) technique in the early 1970s [Kaimal *et al.*, 1972; Garratt, 1975], CO₂ flux has been measured widely over terrestrial ecosystems, for the understanding of temporal

and spatial patterns of CO₂ exchange between terrestrial biospheres and the atmosphere [Baldocchi *et al.*, 1988]. Along with the development of reliable instruments and secure research environments for buoys, ships, and piers, EC has been applied for oceanic flux measurements [Iwata *et al.*, 2004; McGillis *et al.*, 2004; Kondo and Tsukamoto, 2007; Miller *et al.*, 2010; Reimer *et al.*, 2013]. However, partly because of difficulties in accessibility and maintenance, EC measurements over the ocean have generally been quite limited in space and time. Long-term EC measurements over terrestrial ecosystems often show CO₂ fluxes at interannual scale are related to long-term climatic variations, such as the Pacific Decadal Oscillation and the El Niño and La Niña cycle [Saigusa *et al.*, 2005; Wharton *et al.*, 2012; Ueyama *et al.*, 2014]. CO₂ flux over marine ecosystems is also likely to be influenced by long-term climate variability, though information is still quite limited [Feely *et al.*, 1999].

This study reports one of the few long-term data sets for coastal ocean fluxes, employing the EC technique since 2005 at the Scripps pier of the Scripps Institution of Oceanography, University of California, San Diego. About 1.5 km south of the study site is a large kelp forest (the La Jolla kelp bed) that most likely influences EC measurements. It is known that the net ecosystem production of the beach zone of the Southern California Bight is highly influenced by kelp populations and physiology [Zobell, 1971; Steneck *et al.*, 2003; Skadberg, 2009]. Obtained CO₂ flux data were evaluated to help explain the effects of physical and biological coastal processes on the variations of CO₂ flux at different temporal scales in the temperate nearshore water of southern California.

2. Materials and Methods

2.1. Site Description

The Scripps pier (N 32°52.0', W 117°15.4') is located within the Southern California Bight (SCB) coastal region (Figure 1). The California Current flows southward alongshore, but the current is largely mixed, with various local currents in the nearshore surf zone [Bray *et al.*, 1999]. Studies of biological communities in the SCB over the last century have revealed that the SCB is characterized by extensive kelp beds, dominated by *Macrocystis pyrifera* [Dayton *et al.*, 1984; Edwards and Estes, 2006]. The La Jolla kelp bed resides 1.5 km south of the Scripps pier. About 10 km south from the Scripps pier is the Point Loma kelp bed, one of the largest kelp beds in the SCB [MBC Applied Environmental Sciences, 2012].

Northwest onshore winds dominated in summer, and offshore winds became relatively frequent in winter during 2005–2011. The average annual rainfall during the measurement period was 227 mm, which is slightly less than the typical annual rainfall of 262 mm measured at the San Diego international airport from 1981 to 2010 (rainfall data from the Climate Research Division of Scripps Institution of Oceanography).

2.2. Air-Sea CO₂ Flux Measurements From the Scripps Pier

Continuous measurements of CO₂ flux began at the Scripps pier in December 2004. The pier extends 330 m offshore from the beach, and is elevated 11 m above the mean sea surface. A three-dimensional sonic anemometer (WindMaster Pro, Gill Instruments Ltd., UK) and an open-path infrared gas analyzer (LI-7500, LI-COR Biosciences, USA) were mounted on a boom and located at the end of the pier. Measurements were halted periodically due to system maintenances or power failures, and the system operated properly 65% of the time from 2005 to 2011.

Density of CO₂ and H₂O, three-dimensional wind components, and sonic temperature were recorded at 10 Hz and stored on a computer's hard drive at the pier. The computation of eddy covariance was performed half-hourly, following Ikawa *et al.* [2013]. Density correction due to sensor heating increased CO₂ flux by 0.039 g C m⁻² h⁻¹ [Burba *et al.*, 2008]. Corrections for angle of attack for the WindMaster Pro sonic anemometer [Nakai and Shimoyama, 2012] as well as frequency [Moore, 1986] were also applied. These corrections increased the magnitude of CO₂ flux by 17% and 3%, respectively. Low quality data were identified by the following steps and removed: (1) incomplete 30 min data set (1%; hereafter, numbers in parentheses are the percentage of data removed by each step); (2) apparently low signals of instruments as indicators of contamination on the sensor or power failure (3%); (3) wind direction (nonocean source wind, 53%); and (4) 5% of high positive outliers (> 0.14 g C m⁻² h⁻¹) and high negative outliers (< -0.40 g C m⁻² h⁻¹) of CO₂ flux (10%). A footprint analysis [Schuepp *et al.*, 1990] indicated that 90% of the flux originated within 2.5 km off the shore. All algorithms for computing EC data and quality controls were coded with MATLAB ver. 7.4.0 (The MathWorks, Inc., USA).

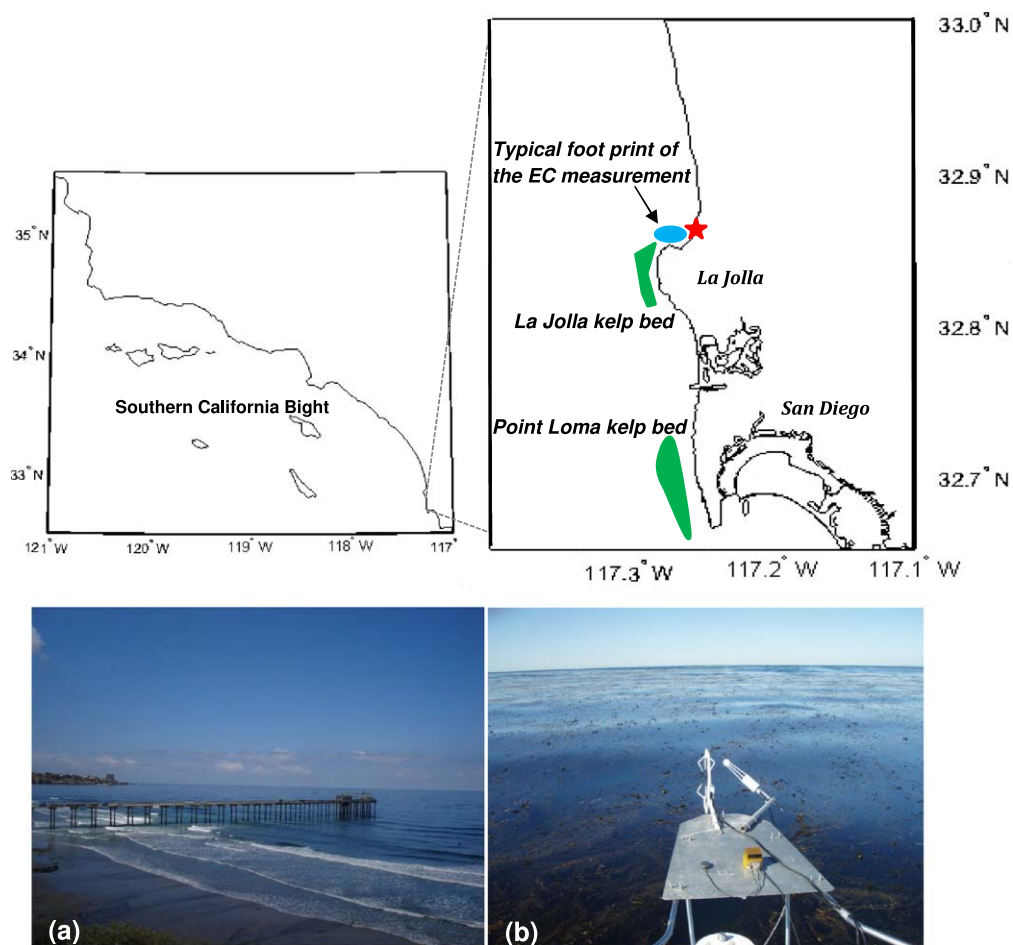


Figure 1. The location of the Scripps pier (star mark) (N 32° 52.0', W 117° 15.4') and major adjacent kelp beds in San Diego, California, USA. (a) The Scripps pier at the Scripps Institution of Oceanography, University of California San Diego (b) Boat-based eddy covariance system used over the Point Loma kelp bed.

2.3. Air-Sea CO₂ Flux Measurement From a Boat

An eddy covariance system was installed on a 15 m long boat to measure CO₂ flux over the Point Loma kelp bed (N 32° 40', W 117° 15') (Figure 1). Measurements were taken 19 May (16:30–17:00 PST), 10 December (12:00–16:00 PST), and 23 December (13:30–15:30 PST) in 2009 and 23 December (12–15:30 PST) in 2011. A sonic anemometer (C-SAT; Campbell Sci., USA), infrared gas analyzer (LI-7500, LI-COR Biosciences, USA), and inertial system (NAV420CA; Crossbow Technology, Inc., USA) were installed on the bow of the boat. Sensors were elevated 2.5 m from the sea surface. The density of CO₂ and H₂O, three-dimensional wind components, sonic temperature, and information from the inertial system were recorded at 20 Hz, and data were stored in a compact flash memory of a datalogger (CR1000; Campbell Sci., USA). Information from the inertial system contained three-dimensional angles and angle velocities, three-dimensional translational velocities, and geographical coordinates. CO₂ flux measured by the boat-based system was calculated in the same manner as data from the Scripps pier, except for the following two steps: (1) 3-D wind speeds were corrected by the inertial system [Edson *et al.*, 1998], and (2) averaging time of CO₂ flux was determined to be 15 min, to ensure that the position and direction of the boat did not change significantly over each averaging window. The use of 15 min averaging time was checked as reasonable for measurements based on the Ogive function [Foken and Wichura, 1996].

2.4. Surface Area of the La Jolla Kelp Bed

MBC Applied Environmental Sciences [2012] reported historical records of kelp bed surface areas, estimated by aerial photographs in southern California. The surface area of the La Jolla kelp bed was reported annually, and 2005–2011 data were used in this study (Figure 39 in the report).

2.5. Climatological and Oceanographic Parameters

To identify coastal processes that control temporal variations of CO₂ flux, climatological and oceanographic parameters were obtained and compared with CO₂ flux. The surface area of the La Jolla kelp bed, reported annually, was also compared with CO₂ flux for investigating interannual variations in CO₂ flux. Climatological and oceanographic parameters used in this study are air temperature, wind speed along prevailing wind direction, friction velocity, chlorophyll concentration, sea surface salinity, sea surface temperature (SST), photosynthetically active photon flux density (PPFD), alongshore wind velocity (AWV), and ENSO index. AWV is considered to induce coastal upwelling, regulating CO₂ outgassing in some coastal zones [Torres *et al.*, 1999; Ikawa *et al.*, 2013]. ENSO index indicates El Niño conditions and La Niña conditions with large positive and negative values, respectively.

Air temperature was estimated from sonic temperature and H₂O mixing ratio every 30 min. Wind speed along prevailing wind direction and friction velocity were calculated from sonic anemometer data every 30 min. Hourly data of chlorophyll concentration, SST, and sea surface salinity were obtained from the Southern California Coastal Ocean Observing System (SCCOOS, <http://www.sccoos.org>) at the Scripps Institution of Oceanography. Hourly PPFD data were obtained from the Climate Research Division of the Scripps Institution of Oceanography (<http://meteora.ucsd.edu>). AWV was calculated based on wind speed and wind direction obtained from the sonic anemometer, assuming that the overall coastal line at the study area is oriented at 315°. ENSO index was obtained from the National Weather Service Climate Prediction Center (<http://www.cpc.ncep.noaa.gov/>).

2.6. Time Series Analysis

All data were decomposed into annual, monthly, daily, and hourly components as follows:

$$P_{obs} = P_Y + P_M + P_D + P_H, \quad (1)$$

where P_{obs} is observed data, P_Y annual components, P_M monthly components, P_D daily components, and P_H hourly components. P_Y is annual average data, P_M was calculated by subtracting monthly average data from annual average data, P_D by subtracting daily average data from monthly average data, and P_H by subtracting observed data from daily average data. Prior to averaging, gaps in the data were filled with average of each hour in each month.

A forward stepwise linear regression was applied to each data set with different temporal components, to identify which parameters among climatological and oceanographic data well explained CO₂ flux at each time scale (i.e., interannual, monthly, daily, and hourly). The statistical level of significance was set at $p < 0.05$. As discussed in Reimer *et al.*, [2013], the influences of various coastal processes on CO₂ flux may not necessarily be linear. Nonetheless, we used linear regressions, as there is no well-defined function to describe relations between CO₂ flux and coastal processes. Air-sea gas transfer can occur independently from the chemical process within seawater, and there can be a lag between CO₂ flux and relevant coastal processes [Reimer *et al.*, 2013]. However, no systematic lag between CO₂ flux and environmental parameters was detected by a cross-correlation analysis in our data set with maximum time lag of 24 hours. Data sets for daily and hourly components were divided every month and every 3 months, respectively, for the regression analysis.

A correlation matrix was calculated for CO₂ flux and climatological and oceanographic parameters, to investigate how environmental parameters were interrelated for each temporal scale. The *Macrocystis* lifespan is about several months to a year [North, 1961; Van Tussenbroek, 1989]. We therefore hypothesized that CO₂ uptake in the current year reflects kelp biomass in the following year, and the surface area of the La Jolla kelp bed in the following year was included in the correlation matrix for interannual variations. All statistical analyses were coded with MATLAB ver. 7.4.0 (The MathWorks, Inc., USA).

2.7. Error Analysis

More than half of the EC data (67%) were filtered out due to nonocean source winds or low data quality, and the potential bias introduced by the discontinuity of the data was concerned for averaging flux over longer periods (monthly and annually). Particularly, winter months (November–February) experienced frequent offshore winds, and about 70% of the data were filtered out.

To evaluate how errors related to the discontinuity of the data acquisition as well as possible noise in the sensors affected the results, the flux data set was reconstructed with random errors and subsequent data analyses were performed 100 times.

Monthly average flux with random errors, F_{M+e} , is written as follows:

$$F_{M+e} = F_M + e_M, \tag{2}$$

where F_M is a monthly average flux and e_M is a random error component. The random error component, e_M , is randomly generated (with Matlab's *normrnd* function) assuming the normal distribution of the error with zero mean and standard deviation of flux for each month, σ_M , viz.

$$e_M = \text{normrnd}(0, \sigma_M). \tag{3}$$

The standard deviation of each month, σ_M , is computed by first calculating standard deviation for each hour of the day (1–24 h) prior to the gap-filling, σ_H , and then averaging σ_H following the rule for error propagation [Taylor, 1982], viz.

$$\sigma_M = \sqrt{\sum_{H=1}^{24} \sigma_H^2 / 24} = \sqrt{[\sigma_1^2 + \sigma_2^2 + \dots + \sigma_{24}^2] / 24}. \tag{4}$$

Annual average flux with random errors, F_{Y+e} , was similarly calculated by the set of the following equations:

$$F_{Y+e} = F_Y + e_Y, \tag{5}$$

$$e_Y = \text{normrnd}(0, \sigma_Y), \tag{6}$$

$$\sigma_Y = \sqrt{\sum_{M=1}^{12} \sigma_M^2 / 12} = \sqrt{[\sigma_1^2 + \sigma_2^2 + \dots + \sigma_{12}^2] / 12}, \tag{7}$$

where F_Y is annual average flux, e_Y random error component, and σ_Y standard deviation of flux for each year.

3. Results

3.1. Climatological and Oceanographic Conditions

Monthly average air temperature and SST ranged from 12°C to 22.5°C and 13°C to 22°C, respectively except for the year 2010 when the maximum monthly air temperature and SST reached only to 19°C and 18°C (Figures 2 and 3). PPF was also lower in 2010 than other years. Wind speeds and friction velocity were relatively high in late winter to early spring, particularly in 2006 and 2007. The highest ENSO index was recorded in the winter of 2009–2010, indicating El Niño conditions occurred.

3.2. Surface Area of the La Jolla Kelp Bed

MBC Applied Environmental Sciences [2012] reported that the surface areas of kelp beds in the extensive coastal zones of southern California, estimated for 1967–2011, were tightly related to the ENSO index. The surface area of the La Jolla kelp bed was largest (4.2 km²) in 2008, while the lowest monthly ENSO index was observed in January and February of 2008. There was no detectable kelp surface area in 2006. The ENSO index was not particularly high or low in 2005–2006, but a moderate El Niño prevailed in the summer–winter of 2004, with the average NINO of 0.7 (data not shown).

3.3. CO₂ Flux and Time Series Analysis

Overall, the study area was a CO₂ sink, with average CO₂ flux of $-260 (\pm 42 \text{ SE}) \text{ g C m}^{-2} \text{ yr}^{-1}$ (Figure 4). Strong sinks of CO₂ (hourly CO₂ flux lower than $-0.2 \text{ g C m}^{-2} \text{ h}^{-1}$) were often observed in summer, with minimum monthly CO₂ flux of $-114 \text{ g C m}^{-2} \text{ month}^{-1}$ in June 2007. Annual CO₂ flux dropped as low as $-575 (\pm 43 \text{ SE}) \text{ g C m}^{-2} \text{ yr}^{-1}$ in 2007. Only during 2005 was there an annual CO₂ source with CO₂ flux of $+27 (\pm 21 \text{ SE}) \text{ g C m}^{-2} \text{ yr}^{-1}$. Monthly components of CO₂ flux were generally low in summer, contributing to CO₂ sinks, and high in winter, contributing to CO₂ sources. No apparent pattern was found in the daily and hourly temporal components of CO₂ flux, as they were highly scattered.

Time series analysis showed that temporal variations in CO₂ flux were related to different environmental parameters at different temporal scales. Interannual variations in CO₂ flux were not explained by any independent parameters; however, annual CO₂ flux reflected the surface area of the La Jolla kelp bed in the following year ($R = -0.93, p < 0.05$) (Table 1, Figure 5a). There was also a strong correlation between ENSO

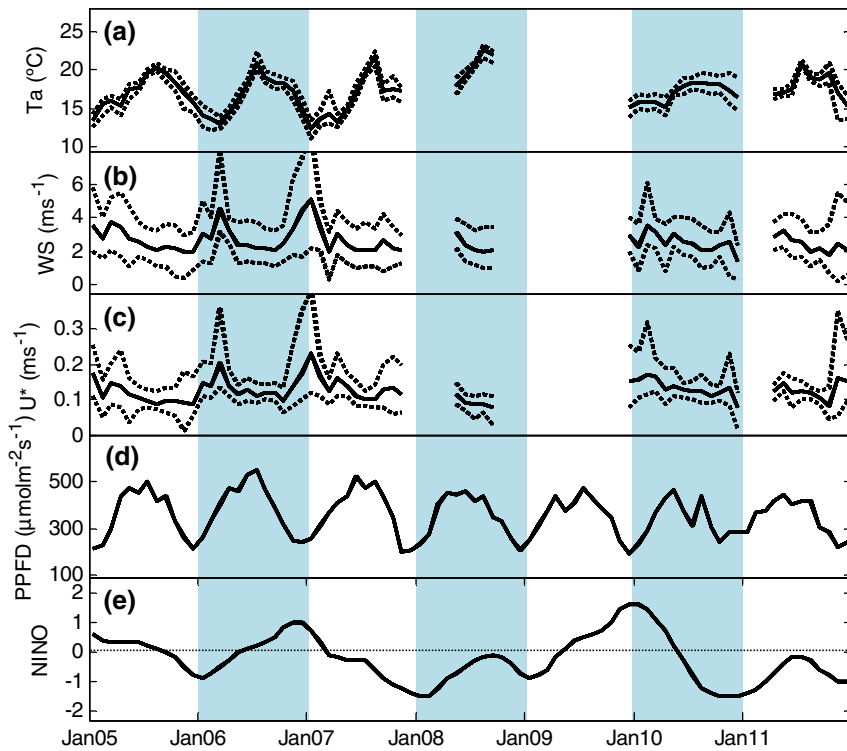


Figure 2. Monthly averages of climatological parameters: (a) air temperature (T_a), (b) wind speed (WS), (c) friction velocity (U^*), (d) photosynthetically active photon flux density ($PPFD$), and (e) ENSO Index ($NINO$). Dotted lines show average daily maximum and minimum for each month. $PPFD$ data were obtained from the Climate Research Division of the Scripps Institution of Oceanography. $NINO$ data were obtained from the National Weather Service, Climate Prediction Center.

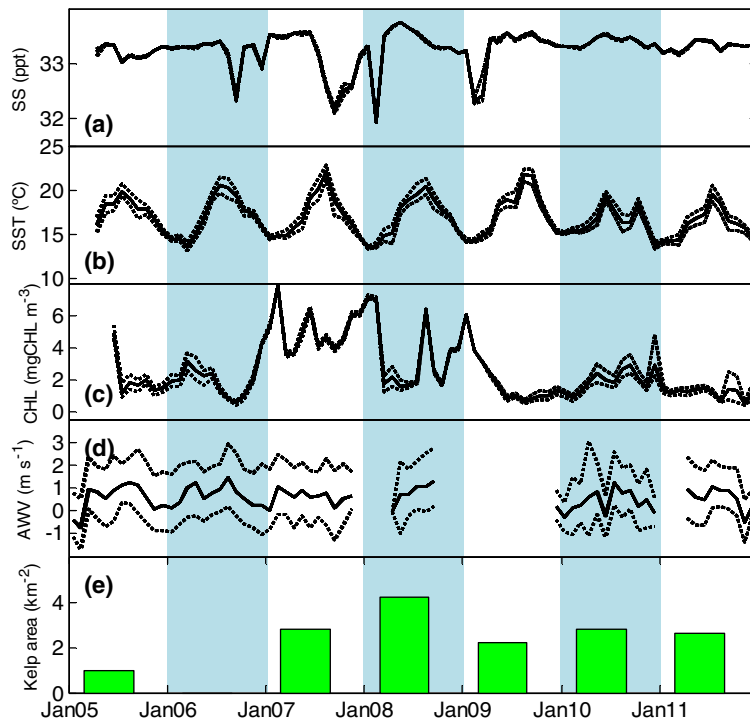


Figure 3. Monthly averages of oceanographic parameters: (a) sea surface temperature (SST), (b) chlorophyll concentration (CHL), (c) sea surface salinity (SS), (d) alongshore wind velocity (AWV), and (e) the surface area of the La Jolla kelp bed. Dotted lines show average daily maximum and minimum for each month. SST , SS , and CHL data were obtained from the Coastal Observing Research and Development Center at the Scripps Institution of Oceanography. The kelp data were obtained from *MBC Applied Environmental Sciences* [2012].

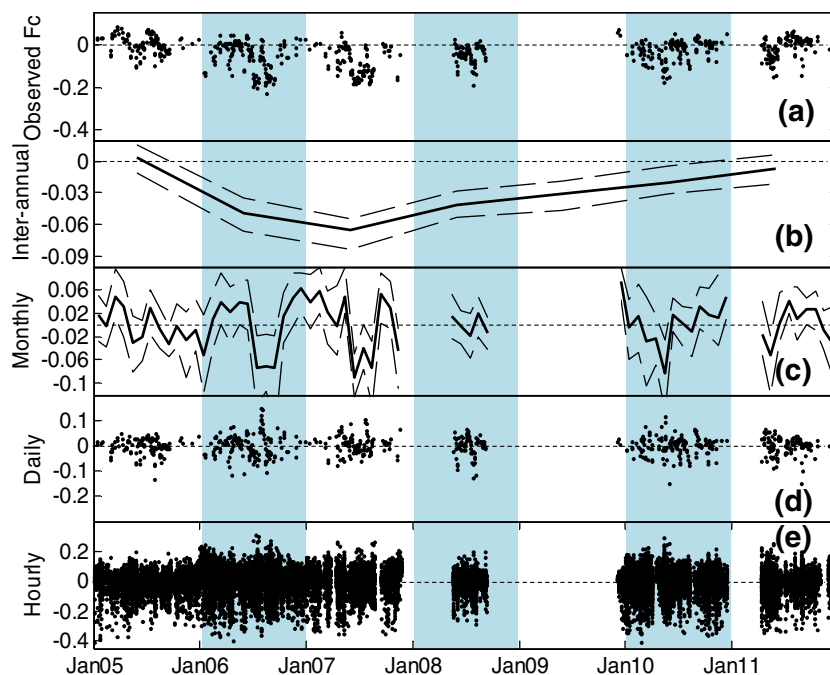


Figure 4. Observed CO₂ flux (F_c) ($\text{g C m}^{-2} \text{h}^{-1}$) and the decomposed temporal variations ($\text{g C m}^{-2} \text{h}^{-1}$) measured by eddy covariance from 2005 through 2011 at the Scripps pier (N 32°52.0', W 117°15.4') near San Diego, California. (a) Observed daily CO₂ flux, (b) interannual variability (annual average), (c) monthly variability, (d) daily variability, and (e) hourly variability. Dashed lines show the maximum and minimum fluxes with random errors.

index and surface area of the kelp bed (Figure 5b). Monthly variations in CO₂ flux were explained by monthly variations in PPF and wind speeds ($R = 0.44$, $p < 0.05$) (Figure 6). Although the monthly component of air temperature was negatively correlated to CO₂ flux ($R = -0.28$, $p < 0.05$), adding air temperature to the regression model did not increase the explanatory power for CO₂ flux, likely due to a strong correlation between air temperature and wind speeds ($R = -0.62$, $p < 0.05$) (Table 1). There was no explainable correlation between daily components of CO₂ flux and environmental parameters (data not shown). Hourly components of CO₂ flux were often negatively correlated to wind speeds as opposed to the positive correlation on a monthly scale (Figure 7).

3.4. Boat-Based EC Measurements

The boat-based eddy covariance measurement over the Point Loma kelp bed showed consistently negative CO₂ flux, ranging from -0.09 to -0.01 $\text{g C m}^{-2} \text{h}^{-1}$ (Figure 8). We were not able to relate the variation in CO₂ flux observed from the boat with environmental conditions; however, the magnitude of the CO₂ sink was similar to the overall average of the CO₂ sink observed at the Scripps pier. The annual average of CO₂ flux observed at the Scripps pier was -260 $\text{g C m}^{-2} \text{yr}^{-1}$, which is equivalent to -0.03 $\text{g C m}^{-2} \text{h}^{-1}$.

3.5. Error Analysis

The stepwise regression analysis on the monthly components with random errors also determined wind speed and PPF are two most important parameters for CO₂ flux at a monthly scale (Figure 9a). They were determined to be important for only 47% and 39% of the total trial due to large potential errors, however. Correlation coefficients (R) for annual CO₂ flux with random errors and the La Jolla kelp bed in the following year varied from -0.98 to -0.84 at $p < 0.05$ (Figure 9b).

4. Discussion

4.1. Temporal Variations

High CO₂ sinks, concurrent with high PPF at monthly scale, as well as high CO₂ sinks at high winds when the sink strength was relatively high on an hourly scale, suggest that the temporal variability in CO₂ flux was mainly biologically driven. A significant correlation between CO₂ flux and the surface area of the La

Table 1. Correlation Coefficients (R) for (a) Monthly Variations (Monthly Average – Annual Average) and (b) Interannual Variations (Annual Average) of CO₂ Flux (F_c), Air Temperature (T_a), Wind Speed (WS), Friction Velocity (U*), PPFD, Sea Surface Salinity (SS), Sea Surface Temperature (SST), Chlorophyll Concentration (CHL), Alongshore Wind Velocity (AWV), ENSO Index, Surface Area of the La Jolla Kelp Bed (Kelp), and Surface Area of the La Jolla Kelp Bed in the Following Year (Kelp (+1))^a

Monthly Variations	Fc	Ta	WS	U*	PPFD	SS	SST	CHL	AWV	NINO		
Fc	1											
Ta	-0.28	1										
WS	0.33	-0.62	1									
U*	0.28	-0.73	0.88	1								
PPFD	-0.32	0.37	-0.18	-0.28	1							
SS	0.12	-0.38	0.23	0.21	0.11	1						
SST	-0.31	0.81	-0.42	-0.53	0.59	-0.21	1					
CHL	0.16	-0.07	0.23	0.13	-0.05	0.11	-0.16	1				
AWV	-0.12	0.39	-0.23	-0.36	0.52	0.05	0.30	0.13	1.00			
NINO	0.09	-0.11	0.33	0.31	0.03	0.14	0.02	-0.07	0.05	1		
Interannual Variations	Fc	Ta	WS	U*	PPFD	SS	SST	CHL	AWV	NINO	KELP	KELP (+1)
Fc	1											
Ta	0.14	1										
WS	-0.28	-0.78	1									
U*	-0.28	-0.88	0.61	1								
PPFD	-0.66	-0.43	0.82	0.38	1							
SS	0.49	0.52	-0.66	-0.32	-0.77	1						
SST	-0.05	-0.17	0.48	-0.26	0.43	-0.63	1					
CHL	-0.78	-0.02	-0.01	-0.02	0.33	-0.56	0.31	1				
AWV	-0.52	0.55	-0.03	-0.48	0.51	-0.28	0.22	0.38	1			
NINO	0.09	-0.60	0.83	0.28	0.48	-0.35	0.65	-0.21	-0.48	1		
KELP	-0.13	0.66	-0.90	-0.46	-0.60	0.44	-0.44	0.40	0.58	-0.87	1	
KELP(+1)	-0.93	-0.15	0.18	0.26	0.45	-0.28	0.01	0.77	0.84	-0.05	0.24	1

^aCorrelations with statistical significance ($p < 0.05$) are listed in bold numbers.

Jolla kelp bed suggests the possibility of biological carbon uptake as largely due to kelp growth, as discussed in the following section. High alongshore wind stress can both induce coastal upwelling and release CO₂ to the atmosphere [Torres et al., 1999; Ikawa et al., 2013]. However, AWV was not determined to be an important parameter at any temporal scales, and high wind speeds simply increased air-sea gas transfer and enhanced CO₂ uptake from the ocean on an hourly scale. Therefore, the influence of the outgassing due to upwelling on CO₂ flux was not detected at this study site unlike other coastal upwelling zones [Torres et al., 1999; Ikawa et al., 2013; Reimer et al., 2013].

Decomposed time series showed that dominant environmental parameters explaining the variation in CO₂ flux were different at different temporal scales, suggesting the importance of long-term monitoring for accurately evaluating coastal processes related to CO₂ flux. Interestingly, wind speeds at a monthly scale were positively correlated to CO₂ flux, as opposed to negative correlation on an hourly scale. The positive correlation between wind speed and CO₂ flux at a monthly scale was not due to upwelling as AWV was not an important determinant for CO₂ flux at our study site (Table 1), and we could not identify the mechanistic reason for the positive correlation. However, our results still suggest that the direction (positive or negative)

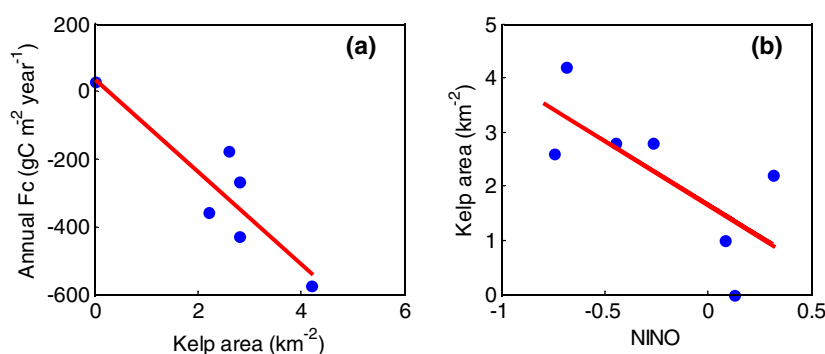


Figure 5. (a) Annual CO₂ flux was correlated to the surface area of the La Jolla kelp bed in the following year ($R = -0.93$, $p < 0.05$), (b) the surface area of the La Jolla kelp bed and the ENSO index (NINO) were negatively correlated ($R = -0.87$, $p < 0.05$).

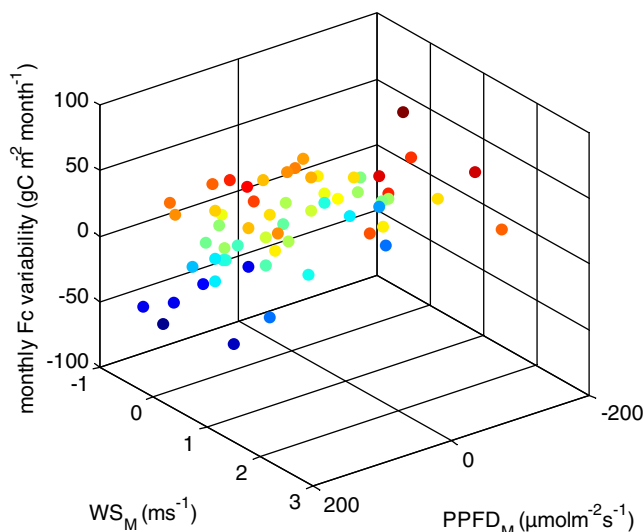


Figure 6. The monthly variability of CO₂ flux (monthly CO₂ flux-annual CO₂ flux) was best correlated to the monthly variability of photosynthetically active photon flux density (PPFD_M) and wind speed (WS_M) ($R = 0.44, p < 0.05$).

of the correlations between environmental parameters and CO₂ flux can be different at different temporal scales.

4.2. Kelp Forest CO₂ Uptake

The overall sink for CO₂ in the study area was most likely due to carbon sequestration by adjacent kelp beds. The lowest annual CO₂ flux of $-575 (\pm 43 \text{ SE}) \text{ g C m}^{-2} \text{ yr}^{-1}$ was recorded in 2007, while the largest surface area of the La Jolla kelp bed (4.2 km^{-2}) was recorded in 2008, inferring that high primary productivity in 2007 led to the large 2008 kelp area. An incubation experiment with individual kelp showed high reductions in pCO₂ in seawater during their active growing period (M. Edwards,

San Diego State University, personal communication, 2014). There was no detectable kelp surface area in 2006 after the highest annual net CO₂ flux of $28 (\pm 81 \text{ SE}) \text{ g C m}^{-2} \text{ yr}^{-1}$ recorded in 2005. Although there was no large kelp bed within the footprint of the EC measurements, our results suggest that the study area was highly influenced by kelp production. Boat-based EC measurements over the Point Loma kelp bed showed similar magnitudes of CO₂ uptake, although the sampling period was too short (a few hours) to evaluate similarity to the Scripps site. Further study is preferred for investigating the spatial extent to which the kelp production induced high CO₂ uptake similarly to our site along the coast.

The temporal patterns of the kelp bed were related to ENSO index, as they showed a negative correlation ($R = -0.95, p < 0.05$). The surface area of the La Jolla kelp bed was largest in 2008, when the ENSO index was lowest. El Niño conditions generally limit the growth of kelp, as these conditions suppress upwelling, which conveys nutrients to the ocean surface [Tegner and Dayton, 1991; Dayton et al., 1998; Edwards and Estes, 2006]. In southern California, El Niño is also associated with low pressure and local storms, which physically reduce the extent of kelp stands [Edwards, 2004]. The surface areas of kelp beds in extensive areas of southern California, recorded in 1967–2011, were also tightly related to the El Niño and La Niña cycle [MBC Applied Environmental Sciences, 2012]. While our results suggest that kelp growth resulted in

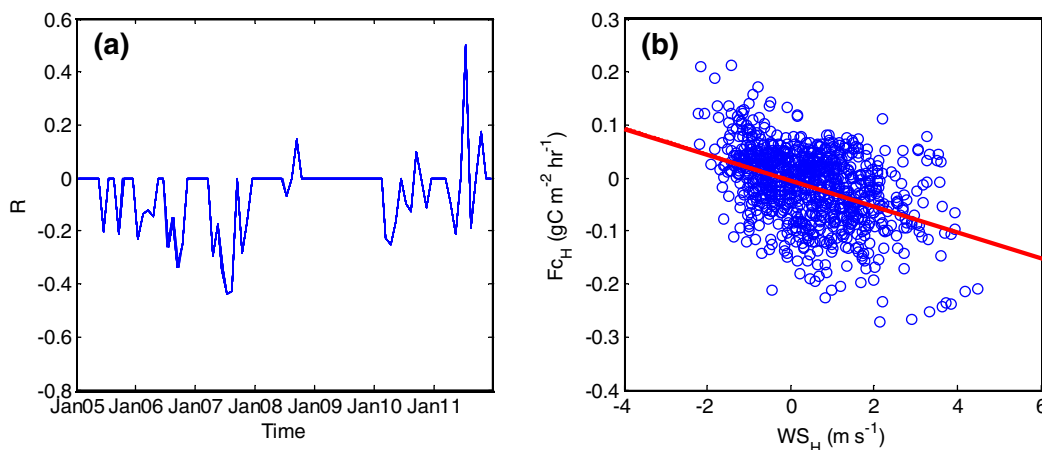


Figure 7. (a) Correlation coefficient (R) between hourly components of CO₂ flux and wind speeds and (b) the relationship between hourly components of CO₂ flux (F_{c_H}) and wind speeds (W_{S_H}) ($F_{c_H} (\text{g C m}^{-2} \text{ h}^{-1}) = -0.02W_{S_H} - 0.003, p < 0.05$) in July 2007.

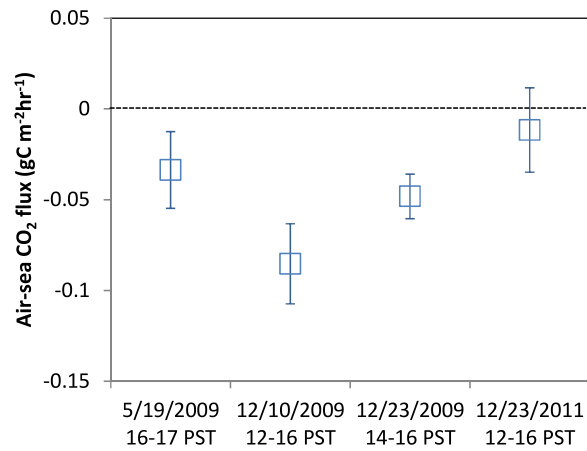


Figure 8. CO₂ flux (g C m⁻² h⁻¹) measured by eddy covariance from the boat over the Point Loma kelp bed (N 32° 40', W 117° 15') near San Diego California.

average ocean CO₂ uptake of ca. 4 g C m⁻² yr⁻¹, based on *Takahashi et al.* [2009], and more than an order higher than the average CO₂ uptake from the global coastal sea of ca. 13 g C m⁻² yr⁻¹, based on *Chen and Borges* [2009]. This sink strength would have a considerable influence on the global carbon cycle if a similar sink strength was to be expected from other macrophyte ecosystems. Reported net primary productivity of large kelps ranges from 300 to 1000 g C m⁻² yr⁻¹ [*Smith, 1981; Duarte and Cebrian, 1996; Wilmers et al.,*

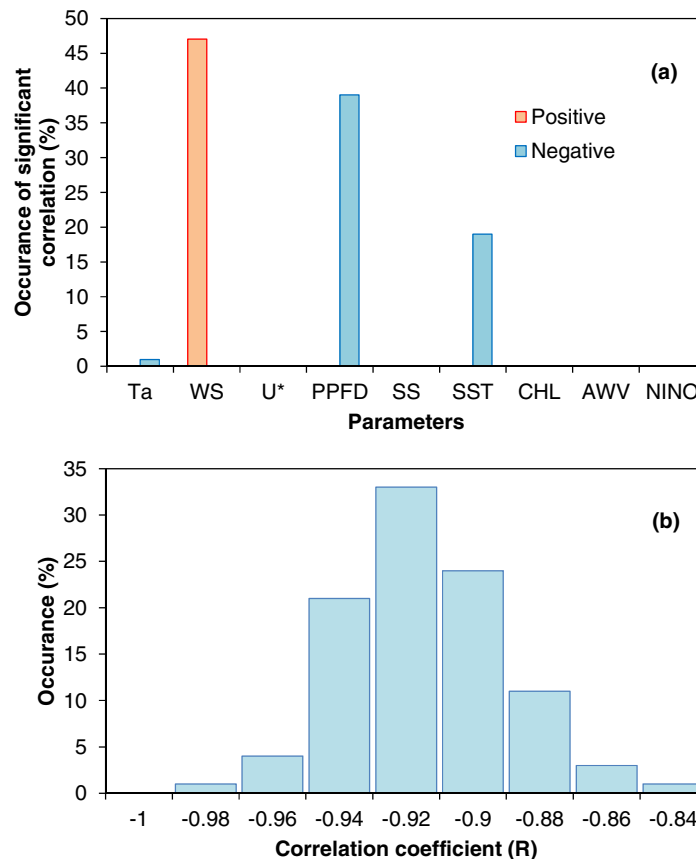


Figure 9. (a) Occurrences of significant correlations between monthly CO₂ flux with random errors and environmental parameters, and (b) occurrence of correlation coefficient (R) between annual CO₂ flux with random errors and the surface area of the La Jolla kelp bed in the following year.

high CO₂ uptake and increased the surface area of the La Jolla kelp bed the following year, no correlation was found between either CO₂ flux and the ENSO index or the ENSO index and the kelp bed area during the following year. Further investigation is necessary to identify which life stage of the kelp is sensitive to PPFd or El Niño/La Niña conditions for kelp growth.

Overall, the study area was a strong sink for CO₂ over the 7 year period, with an average annual CO₂ flux of -260 (±42 SE) g C m⁻² yr⁻¹. This sink strength is almost two orders of magnitude higher than the global

average ocean CO₂ uptake of ca. 4 g C m⁻² yr⁻¹, based on *Takahashi et al.* [2009], and more than an order higher than the average CO₂ uptake from the global coastal sea of ca. 13 g C m⁻² yr⁻¹, based on *Chen and Borges* [2009]. This sink strength would have a considerable influence on the global carbon cycle if a similar sink strength was to be expected from other macrophyte ecosystems. Reported net primary productivity of large kelps ranges from 300 to 1000 g C m⁻² yr⁻¹ [*Smith, 1981; Duarte and Cebrian, 1996; Wilmers et al.,*

2012], which would be similar to net primary productivity at our site if the ecosystem respiration was approximated by the highest CO₂ source. Although macrophyte ecosystems have relatively less storage within floor sediment compared to sea grass [*Duarte and Cebrian, 1996; Fourqurean et al., 2012*], sequestered CO₂ in macrophyte ecosystems are effectively exported to the deep ocean, enhancing new production [*Smith, 1981; Duarte and Cebrian, 1996*]. If the whole coastal sea inhabited by macrophytes (2 × 10⁶ km²) had a similar strength CO₂ uptake, net CO₂ uptake from these ecosystems would be estimated at 0.5 Pg C yr⁻¹, which is roughly equal to the net CO₂ sink currently estimated for the entire global coastal ocean, and 30% of the net sink of the global ocean estimated to-date.

To our knowledge, there are few studies that use EC for coastal seas possibly inhabited by macrophytes [*Ikawa et al.,*

2013; Reimer *et al.*, 2013]. However, EC systems used by Ikawa *et al.* [2013] and Reimer *et al.* [2013] were located in the intertidal areas, where a CO₂ release induced by breaking waves likely masked the influence of CO₂ uptakes by macrophytes. Since estimations of CO₂ flux by an indirect method such the bulk method based on pCO₂ measurements are particularly difficult over macrophyte ecosystems, due to the large uncertainty in the air-sea gas transfer property [Delille *et al.*, 2009], more direct measurements, such as the EC technique, are necessary for quantifying CO₂ flux in these ecosystems.

Ecosystems dominated by macrophytes are not necessarily a CO₂ sink, particularly if coastal upwelling currents are dominant [Friederich *et al.*, 2002; Wilkerson *et al.*, 2006; Ikawa *et al.*, 2013; Reimer *et al.*, 2013]. Nonetheless, the sink strength of macrophytes likely affects net CO₂ flux considerably in coastal upwelling ecosystems as well, as the potential reported in this study and by others such as Smith [1981] and Wilmers *et al.* [2012] for kelp primary production to take up CO₂ is comparable to the magnitude of the CO₂ source in an intense upwelling zone (CO₂ flux in coastal upwelling is summarized in Ikawa *et al.* [2013]).

4.3. Future Trajectories of Air-Sea CO₂ Flux Over Macrophyte Ecosystems

The mechanistic understanding of CO₂ flux in our study will help predict the future trajectory of the coastal carbon cycle. Our study suggests that the temporal variation in CO₂ flux near the kelp bed is directly influenced by the primary productivity of kelp beds. While our results did not show any evidence of direct influences from the El Niño and La Niña cycle on CO₂ flux, their influences on CO₂ flux may be revealed on a much longer temporal scale, as El Niño conditions often restrict kelp growth. Future projections of the El Niño and La Niña cycle still cannot be predicted with confidence [Meehl *et al.*, 2006; Guilyardi *et al.*, 2009]. However, frequent storms and extremely high temperatures are expected in the future, in response to climate change, and such El Niño-like conditions will most likely damage macrophyte ecosystems, thus reducing their carbon uptake potential [Alexander *et al.*, 2006; Byrnes *et al.*, 2011; Reed *et al.*, 2011]. The negative effect of extreme climate on primary productivity may be partly offset by the positive effect of increasing coastal upwelling, which conveys nutrients to the sea surface [Bakun, 1990; Snyder *et al.*, 2003; Garcia-Reyes and Largier, 2010].

Macrophyte ecosystems are particularly susceptible to environmental change. Their biomass and physiology are influenced by local climate, nutrient availability, grazing, water quality and physical disturbance [Dayton, 1985; Dayton *et al.*, 1999; Steneck *et al.*, 2003; Edwards, 2004]. Top-down forcing of the food web, particularly, by pollution and grazing, can severely deteriorate kelp forests [Steneck *et al.*, 2003]. Particularly, nonpoint pollution, due mainly to land-use changes, has severely degraded coastal macrophyte ecosystems globally, and is subject to increase in the future [Carpenter *et al.*, 1998; Fourqurean *et al.*, 2012]. Subsequent degradation of macrophyte ecosystems may result in a reduction of one of the world's greatest CO₂ sinks.

4.4. Methodological Uncertainty

The error analysis showed that the EC data set with possible random errors due to sampling bias put out consistent results in the correlation analyses. However, the application of the EC over the ocean still remains some issues to be carefully addressed.

First, ocean EC flux generally has low signal-to-noise ratios [Kondo and Tsukamoto, 2007]. Our EC flux data set also suffered from high temporal variations that were not completely distinguishable from noise, particularly at hourly and daily scales (Figure 4). The error analysis conducted in this study revealed that random errors due to sampling discontinuity as well as potential noise did not affect correlation analyses at monthly and interannual scales. However, we could not identify important environmental parameters that control the daily variation of CO₂ flux likely due to high scatters.

Second, contaminations especially from sea spray on the infrared gas analyzer may cause a false negative correlation between CO₂ and H₂O signals, possibly due to the erroneous change in spectroscopic cross sensitivities of the infrared gas analyzer [Prytherch *et al.*, 2010; Kondo *et al.*, 2014]. We carefully cleaned the instruments weekly basis, and the sensitivity of CO₂ to H₂O in our study was an order magnitude lower than that reported by Prytherch *et al.* [2010]. Therefore, we assumed that the false correlation was not a particular issue for our case. However, it may be recommendable to employ a closed-path infrared gas analyzer and dry the air stream for the application of EC over the ocean for better data quality in future [Miller *et al.*, 2010; Landwehr *et al.*, 2014].

Lastly, CO₂ flux measured by EC often disagree with the estimates from the bulk gradient method [Reimer *et al.*, 2013; Ikawa and Oechel, 2014]. Reimer *et al.* [2013] discussed that the higher magnitudes of CO₂ flux

by EC than expected by the bulk method were due to the fact their EC instruments were located at an intertidal zone where gas transfer can occur at a much higher rate than estimated by the conventional methods developed for open water [e.g., Wanninkhof, 1992]. Our study site located near the shore including the macrophyte ecosystem most likely has different regulations on gas transfer velocity than open water [Delille et al., 2009]; therefore, EC was still more desirable for flux measurements than the bulk method at our study site.

5. Conclusions

This study reports one of the first multiyear observations of air-sea CO₂ flux by the EC for the near-shore waters of San Diego, California. Monthly variations in CO₂ flux were negatively correlated to PPF, suggesting biological CO₂ uptakes. Interannual variations in CO₂ flux were no longer correlated to PPF, but were correlated to the surface area of the La Jolla kelp bed in the following year, suggesting that kelp growth enhanced CO₂ uptakes. While CO₂ uptake was negatively related to wind speeds at a monthly scale, wind speeds affected CO₂ uptake positively on an hourly scale, suggesting the importance of long-term monitoring of CO₂ flux for accurately identifying important environmental processes relevant to the coastal carbon cycle. The study area was, overall, a strong CO₂ sink, and this sink strength may possibly update our understanding of the global carbon budget considerably, if the whole coastal sea inhabited by macrophytes shows a similar CO₂ uptake strength. It should be also noted that the application of EC over the ocean still includes technical difficulties and uncertainties with respect to low signal-to-noise ratio, the uncertain influence of the sensor contamination, and inconsistency with other methods. These issues must be addressed carefully for better EC data quality in future.

Acknowledgments

CO₂ flux data used in this study are obtained as a supporting information as Flux_data_ikawa&Oechel_JGR.csv. Oceanography data were obtained the Southern California Coastal Ocean Observing System (SCCOOS, <http://www.sccoos.org>) at the Scripps Institution of Oceanography. PPF data were obtained from the Climate Research Division of Scripps Institution of Oceanography (<http://meteora.ucsd.edu>). The ENSO index was obtained from the National Weather Service Climate Prediction Center (<http://www.cpc.ncep.noaa.gov/>). Kelp area data were obtained from Michael D. Curtis (MBC Applied Environmental Sciences). We also thank Ralph Keeling for unfailing collaboration at the Scripps pier; Wade McGillis for designing the boom and for consulting on equipment and approach; Christian McDonalds for logistic support; Matthew Edwards for valuable advice on kelp studies; Kirstin Skadberg and Joseph Verfaillie for data collection, system setup, and valuable suggestions; Michelle Kim for her helpful suggestions; and Nate Bauer for editing the manuscript.

References

- Alexander, L. V., et al. (2006), Global observed changes in daily climate extremes of temperature and precipitation, *J. Geophys. Res.*, *111*, D05109, doi:10.1029/2005JD006290.
- Bakun, A. (1990), Global climate change and intensification of coastal ocean upwelling, *Science*, *247*(4939), 198–201, doi:10.1126/science.247.4939.198.
- Baldocchi, D. D., B. B. Hicks, and T. P. Meyers (1988), Measuring biosphere-atmosphere exchanges of biologically related gases with micro-meteorological methods, *Ecology*, *69*(5), 1331–1340.
- Borges, A. (2005), Do we have enough pieces of the jigsaw to integrate CO₂ fluxes in the coastal ocean?, *Estuaries*, *28*(1), 3–27, doi:10.1007/BF02732750.
- Bray, N. A., A. Keyes, and W. M. L. Morawitz (1999), The California Current system in the Southern California Bight and the Santa Barbara Channel, *J. Geophys. Res.*, *104*(C4), 7695–7714, doi:10.1029/1998JC900038.
- Burba, G. G., D. K. McDermitt, A. Grelle, D. J. Anderson, and L. Xu (2008), Addressing the influence of instrument surface heat exchange on the measurements of CO₂ flux from open-path gas analyzers, *Global Change Biol.*, *14*(8), 1854–1876, doi:10.1111/j.1365-2486.2008.01606.x.
- Byrnes, J. E., D. C. Reed, B. J. Cardinale, K. C. Cavanaugh, S. J. Holbrook, and R. J. Schmitt (2011), Climate-driven increases in storm frequency simplify kelp forest food webs, *Global Change Biology*, *17*(8), 2513–2524, doi:10.1111/j.1365-2486.2011.02409.x.
- Cai, W.-J., M. Dai, and Y. Wang (2006), Air-sea exchange of carbon dioxide in ocean margins: A province-based synthesis, *Geophys. Res. Lett.*, *33*, L12603, doi:10.1029/2006GL026219.
- Carpenter, S. R., N. F. Caraco, D. L. Correll, R. W. Howarth, A. N. Sharpley, and V. H. Smith (1998), Nonpoint pollution of surface waters with phosphorus and nitrogen, *Ecol. Appl.*, *8*(3), 559–568, doi:10.1890/1051-0761(1998)008[0559:NPOSWW]2.0.CO;2.
- Chen, C.-T. A., and A. V. Borges (2009), Reconciling opposing views on carbon cycling in the coastal ocean: Continental shelves as sinks and near-shore ecosystems as sources of atmospheric CO₂, *Deep Sea Res., Part II*, *56*(8–10), 578–590, doi:10.1016/j.dsr2.2009.01.001.
- Dayton, P. K. (1985), Ecology of Kelp communities, *Annu. Rev. Ecol. Syst.*, *16*(1), 215–245, doi:10.1146/annurev.es.16.110185.001243.
- Dayton, P. K., V. Currie, T. Gerrodette, B. D. Keller, R. Rosenthal, and D. V. Tresca (1984), Patch dynamics and stability of some California Kelp communities, *Ecol. Monogr.*, *54*(3), 253–289, doi:10.2307/1942498.
- Dayton, P. K., M. J. Tegner, P. B. Edwards, and K. L. Riser (1998), Sliding baselines, ghosts, and reduced expectations in kelp forest communities, *Ecol. Appl.*, *8*(2), 309–322, doi:10.1890/1051-0761(1998)008[0309:SBGARE]2.0.CO;2.
- Dayton, P. K., M. J. Tegner, P. B. Edwards, and K. L. Riser (1999), Temporal and spatial scales of kelp demography: The role of oceanographic climate, *Ecol. Monogr.*, *69*(2), 219–250.
- Delille, B., D. Delille, M. Fiala, C. Prevost, and M. Frankignoulle (2000), Seasonal changes of pCO₂ over a subantarctic *Macrocystis* kelp bed, *Polar Biol.*, *23*(10), 706–716.
- Delille, B., A. V. Borges, and D. Delille (2009), Influence of giant kelp beds (*Macrocystis pyrifera*) on diel cycles of pCO₂ and DIC in the Sub-Antarctic coastal area, *Estuaries Coastal Shelf Sci.*, *81*(1), 114–122.
- Delille, D., G. Marty, M. Cansemi-Soullard, and M. Frankignoulle (1997), Influence of subantarctic *Macrocystis* bed metabolism in diel changes of marine bacterioplankton and CO₂ fluxes, *J. Plankton Res.*, *19*(9), 1251–1264, doi:10.1093/plankt/19.9.1251.
- Duarte, C. M., and J. Cebrian (1996), The fate of marine autotrophic production, *Limnol. Oceanogr.*, *41*(8), 1758–1766.
- Edson, J., A. A. Hinton, and K. E. Prada (1998), Direct Covariance Flux Estimates from Mobile Platforms at Sea, *Am. Meteorol. Soc.*, *15*, 547–561.
- Edwards, M. S. (2004), Estimating scale-dependency in disturbance impacts: El Niños and giant kelp forests in the northeast Pacific, *Oecologia*, *138*(3), 436–447, doi:10.1007/s00442-003-1452-8.

- Edwards, M. S., and J. A. Estes (2006), Catastrophe, recovery and range limitation in NE Pacific kelp forests: A large-scale perspective, *Mar. Ecol. Prog. Ser.*, *320*, 79–87, doi:10.3354/meps320079.
- Feely, R. A., R. Wanninkhof, T. Takahashi, and P. Tans (1999), Influence of El Niño on the equatorial Pacific contribution to atmospheric CO₂ accumulation, *Nature*, *398*(6728), 597–601, doi:10.1038/19273.
- Foken, T., and B. Wichura (1996), Tools for quality assessment of surface-based flux measurements, *Agric. For. Meteorol.*, *78*(1–2), 83–105.
- Fourqurean, J. W., et al. (2012), Seagrass ecosystems as a globally significant carbon stock, *Nat. Geosci.*, *5*, 505–509, doi:10.1038/ngeo1477.
- Friederich, G. E., P. M. Walz, M. G. Burczynski, and F. P. Chavez (2002), Inorganic carbon in the central California upwelling system during the 1997–1999 El Niño-La Niña event, *Prog. Oceanogr.*, *54*(1–4), 185–203.
- García-Reyes, M., and J. Largier (2010), Observations of increased wind-driven coastal upwelling off central California, *J. Geophys. Res.*, *115*, C04011, doi:10.1029/2009JC005576.
- Garratt, J. (1975), Limitations of the Eddy-correlation technique for the determination of turbulent fluxes near the surface, *Boundary Layer Meteorol.*, *8*(3), 255–259, doi:10.1007/BF02153552.
- Gruber, N., et al. (2009), Oceanic sources, sinks, and transport of atmospheric CO₂, *Global Biogeochem. Cycles*, *23*, GB1005, doi:10.1029/2008GB003349.
- Guillyardi, E., A. Wittenberg, A. Fedorov, M. Collins, C. Wang, A. Capotondi, G. J. van Oldenborgh, and T. Stockdale (2009), Understanding El Niño in ocean–atmosphere general circulation models: Progress and challenges, *Bull. Am. Meteorol. Soc.*, *90*(3), 325–340, doi:10.1175/2008BAMS2387.1.
- Ikawa, H., and W. C. Oechel (2014), Spatial and temporal variability of air–sea CO₂ exchange of alongshore waters in summer near Barrow, Alaska, *Estuarine Coastal Shelf Sci.*, *141*, 37–46, doi:10.1016/j.ecss.2014.02.002.
- Ikawa, H., I. Falovina, J. Kochendorfer, K. T. Paw U, and W. C. Oechel (2013), Air–sea exchange of CO₂ at a Northern California coastal site along the California Current upwelling system, *Biogeosciences*, *10*(7), 4419–4432, doi:10.5194/bg-10-4419-2013.
- Iwata, T., K. Yoshikawa, K. Nishimura, Y. Higuchi, T. Yamashita, S. Kato, and E. Ohtaki (2004), CO₂ flux measurements over the sea surface by eddy correlation and aerodynamic techniques, *J. Oceanogr.*, *60*(6), 995–1000.
- Kaimal, J. C., J. C. Wyngaard, Y. Izumi, and O. R. Cote (1972), Spectral characteristics of surface-layer turbulence, *Q. J. R. Meteorol. Soc.*, *98*(417), 563–589.
- Kondo, F., and O. Tsukamoto (2007), Air–sea CO₂ flux by eddy covariance technique in the equatorial Indian Ocean, *J. Oceanogr.*, *63*(3), 449–456.
- Kondo, F., K. Ono, M. Mano, A. Miyata, and O. Tsukamoto (2014), Experimental evaluation of water vapour cross-sensitivity for accurate eddy covariance measurement of CO₂ flux using open-path CO₂/H₂O gas analysers, *Tellus, Ser. B*, *66*, 23803, doi:10.3402/tellusb.v66.23803.
- Landwehr, S., S. D. Miller, M. J. Smith, E. S. Saltzman, and B. Ward (2014), Analysis of the PKT correction for direct CO₂ flux measurements over the ocean, *Atmos. Chem. Phys.*, *14*(7), 3361–3372, doi:10.5194/acp-14-3361-2014.
- MBC Applied Environmental Sciences (2012), *Region Nine Kelp Survey Consortium. 2011 Survey*, prepared for the Region Nine Kelp Survey Consortium, 50 p. plus appendices, Costa Mesa, Calif.
- McGillis, W. R., et al. (2004), Air–sea CO₂ exchange in the equatorial Pacific, *J. Geophys. Res.*, *109*, C08S02, doi:10.1029/2003JC002256.
- Meehl, G. A., H. Teng, and G. Branstator (2006), Future changes of El Niño in two global coupled climate models, *Clim. Dyn.*, *26*(6), 549–566, doi:10.1007/s00382-005-0098-0.
- Miller, S. D., C. Marandino, and E. S. Saltzman (2010), Ship-based measurement of air–sea CO₂ exchange by eddy covariance, *J. Geophys. Res.*, *115*, D02304, doi:10.1029/2009JD012193.
- Moore, C. J. (1986), Frequency response corrections for eddy correlation systems, *Boundary Layer Meteorol.*, *37*(1), 17–35.
- Nakai, T., and K. Shimoyama (2012), Ultrasonic anemometer angle of attack errors under turbulent conditions, *Agric. For. Meteorol.*, *162–163*, 14–26, doi:10.1016/j.agrformet.2012.04.004.
- North, W. J. (1961), Life-span of the Fronds of the Giant Kelp, *Macrocystis pyrifera*, *Nature*, *190*(4782), 1214–1215, doi:10.1038/1901214a0.
- Prytherch, J., M. J. Yelland, R. W. Pascal, B. I. Moat, I. Skjelvan, and C. C. Neill (2010), Direct measurements of the CO₂ flux over the ocean: Development of a novel method, *Geophys. Res. Lett.*, *37*, L03607, doi:10.1029/2009GL041482.
- Reed, D. C., A. Rassweiler, M. H. Carr, K. C. Cavanaugh, D. P. Malone, and D. A. Siegel (2011), Wave disturbance overwhelms top-down and bottom-up control of primary production in California kelp forests, *Ecology*, *92*(11), 2108–2116, doi:10.1890/11-0377.1.
- Reimer, J. J., R. Vargas, S. V. Smith, R. Lara-Lara, G. Gaxiola-Castro, J. M. Hernandez-Ayon, A. Castro, M. Escoto-Rodriguez, and J. Martínez-Osuna (2013), Air–sea CO₂ fluxes in the near-shore and intertidal zones influenced by the California Current, *J. Geophys. Res. Oceans*, *118*, 4795–4810, doi:10.1002/jgrc.20319.
- Sabine, C. L., et al. (2004), The oceanic sink for anthropogenic CO₂, *Science*, *305*(5682), 367–371, doi:10.1126/science.1097403.
- Saigusa, N., S. Yamamoto, S. Murayama, and H. Kondo (2005), Inter-annual variability of carbon budget components in an AsiaFlux forest site estimated by long-term flux measurements, *Agric. For. Meteorol.*, *134*(1–4), 4–16, doi:10.1016/j.agrformet.2005.08.016.
- Sarmiento, J. L., P. Monfray, E. Maier-Reimer, O. Aumont, R. J. Murnane, and J. C. Orr (2000), Sea-air CO₂ fluxes and carbon transport: A comparison of three ocean general circulation models, *Global Biogeochem. Cycles*, *14*(4), 1267–1281, doi:10.1029/1999GB900062.
- Schuepp, P. H., M. Y. Leclerc, J. I. MacPherson, and R. L. Desjardins (1990), Footprint prediction of scalar fluxes from analytical solutions of the diffusion equation, *Boundary Layer Meteorol.*, *50*(1), 355–373.
- Skadberg, K. (2009), Patterns and drivers of nearshore coastal air–sea CO₂ exchange. PhD dissertation, Univ. of Calif., San Diego and Davis, Calif.
- Smith, S. V. (1981), Marine macrophytes as a global carbon sink, *Science*, *211*(4484), 838–840, doi:10.1126/science.211.4484.838.
- Snyder, M. A., L. C. Sloan, N. S. Duffenbaugh, and J. L. Bell (2003), Future climate change and upwelling in the California Current, *Geophys. Res. Lett.*, *30*(15), 1823, doi:10.1029/2003GL017647.
- Steneck, R. S., M. H. Graham, B. J. Bourque, D. Corbett, J. M. Erlandson, J. A. Estes, and M. J. Tegner (2003), Kelp forest ecosystems: Biodiversity, stability, resilience and future, *Environ. Conserv.*, *29*(04), 436–459, doi:10.1017/S0376892902000322.
- Takahashi, T., et al. (2002), Global sea–air CO₂ flux based on climatological surface ocean pCO₂, and seasonal biological and temperature effects, *Deep Sea Res., Part II*, *49*(9–10), 1601–1622, doi:10.1016/S0967-0645(02)00003-6.
- Takahashi, T., et al. (2009), Climatological mean and decadal change in surface ocean pCO₂, and net sea–air CO₂ flux over the global oceans, *Deep Sea Res., Part II*, *56*(8–10), 554–577, doi:10.1016/j.dsr2.2008.12.009.
- Taylor, J. R. (1982), *An Introduction to Error Analysis: The Study of Uncertainties in Physical Measurements*, 372 pp., Univ. Sci. Books, Mill Valley, Calif.
- Tegner, M. J., and P. K. Dayton (1991), Sea urchins, El Niños, and the long term stability of Southern California kelp forest communities, *Mar. Ecol. Prog. Ser.*, *77*(1), 49–63.
- Thomas, H. (2004), Enhanced open ocean storage of CO₂ from shelf sea pumping, *Science*, *304*(5673), 1005–1008, doi:10.1126/science.1095491.

- Torres, R., D. R. Turner, N. Silva, and J. Rutllant (1999), High short-term variability of CO₂ fluxes during an upwelling event off the Chilean coast at 30° S, *Deep Sea Res., Part I*, 46(7), 1161–1179, doi:10.1016/S0967-0637(99)00003-5.
- Tsunogai, S., S. Watanabe, and T. Sato (1999), Is there a “continental shelf pump” for the absorption of atmospheric CO₂?, *Tellus, Ser. B*, 51(3), 701–712, doi:10.1034/j.1600-0889.1999.t01-2-00010.x.
- Van Tussenbroek, B. I. (1989), The life-span and survival of fronds of *Macrocystis pyrifera* (Laminariales, Phaeophyta) in the Falkland Islands, *Br. Phycol. J.*, 24(2), 137–141, doi:10.1080/00071618900650131.
- Ueyama, M., H. Iwata, and Y. Harazono (2014), Autumn warming reduces the CO₂ sink of a black spruce forest in interior Alaska based on a nine-year eddy covariance measurement, *Global Change Biol.*, 20(4), 1161–1173, doi:10.1111/gcb.12434.
- Wanninkhof, R. (1992), Relationship between wind speed and gas exchange over the ocean, *J. Geophys. Res.*, 97(C5), 7373–7382, doi:10.1029/92JC00188.
- Wharton, S., M. Falk, K. Bible, M. Schroeder, and K. T. Paw U (2012), Old-growth CO₂ flux measurements reveal high sensitivity to climate anomalies across seasonal, annual and decadal time scales, *Agric. For. Meteorol.*, 161, 1–14, doi:10.1016/j.agrformet.2012.03.007.
- Whittaker, R. H., and G. E. Likens (1973), Carbon in the biota. edited by G. M. Woodwell, and E. V. Pecan, pp. 281–302, Carbon and the Biosphere. U. S. Atomic Energy Commission. CONF-720510, National Technical Information Service, Springfield, Va.
- Wilkerson, F. P., A. M. Lassiter, R. C. Dugdale, A. Marchi, and V. E. Hogue (2006), The phytoplankton bloom response to wind events and upwelled nutrients during the CoOP WEST study, *Deep Sea Res., Part II*, 53(25-26), 3023–3048.
- Wilmers, C. C., J. A. Estes, M. Edwards, K. L. Laidre, and B. Konar (2012), Do trophic cascades affect the storage and flux of atmospheric carbon? An analysis of sea otters and kelp forests, *Frontiers Ecol. Environ.*, 10, 409–415, doi:10.1890/110176.
- Zobell, C. E. (1971), Drift seaweeds on San Diego county beaches, *Nova Hedwigia*, 32, 269–314.